Performance and potential of a novel floating photovoltaic system in Egyptian climate on calm water surface

*Nabil A.S. Elminshawy [1, *], A.M.I. Mohamed [2], Amr Osama [3], Islam Amin[4], Ameen M. Bassam[5], Erkan Oterkus [6]*
[1,2,3]Mechanical Power Department, Faculty of Engineering, Port-Said University, Egypt
[4,5] Department of Naval Architecture and Marine Engineering, Port Said University, Port Said, Egypt
[6]Department of Naval Architecture, Ocean and Marine Engineering, University of Strathclyde, Glasgow G4 0LZ, United Kingdom

[*]Corresponding author E-mail address: profminshawy@gmail.com Tel.: +201001593131

ABSTRACT

This article investigates the performance of a partially submerged floating photovoltaic system (PSFPV) as a proposal for harvesting solar energy as an electricity production novel system under Egyptian hot climate on calm water surfaces. The proposed system comprised of a floating photovoltaic system with a submerged portion in the surrounding water. The PSFPV system is constructed in addition to the water body and is then extensively examined under Egyptian outdoor conditions. The submerged portion of the PSFPV system keeps the system passively cool by being in direct contact with the surrounding water. A performance comparison between the novel PSFPV system and a similar land-based photovoltaic system (LPV) is also provided. The suggested PSFPV module's thermal and electrical performance was evaluated concerning its submerged length, which ranged from 4 to 24 cm. The results reveal that the PSFPV system achieves a reduction of about 15.10 % in operating temperature relative to the LPV system. Also, the PSFPV system produces up to 20.76% more electricity than the LPV system. The PSFPV system is capable of alleviating the emission of CO_2 by about 49.66 kg/summer season. The proposed PSFPV system reveals a reduction in the LCOE from 0.075 to 0.067 ($/kWh) by increasing the submerged length from 4 to 24 cm.

Keywords: Partially submerged photovoltaic; PSFPV performance; passive cooling; efficiency.

1. Introduction

The world's attention has turned to renewable energy, especially solar energy, as an alternative source because of its potential. Improving the efficiency of photovoltaic cells has become a global trend to rely on PV cells as an alternative, clean energy source [1]. Approximately up to 80% of the solar irradiance received by the PV module is lost as excess heat, with the remainder converted into electricity [2]. The above contributes to a rise in module temperature and, as a result, a decrease in efficiency [3]. Koteswararao et al. [4] clarified that the module's high temperature can

negatively affect the semiconductor utilized to manufacture the module and thus decrease the life of the module and its conversion efficiency. Many approaches, such as active and passive cooling, have been applied to the conventional PV cell to increases its efficiency by reducing the cell temperature studied [5–7]. An external energy supply is necessary for active cooling approaches to dissipate excess heat through the cooling fluid. Sargunanathan et al. [8] give an outline of analytical and experimental research on improving the productivity of PV cells through the use of various cooling strategies. Sajjad et al. [9] carried out experimental research on an air-cooled PV module and compared the results to the PV module with no cooling. According to their findings, the cooling module had a 7.20% and a 6% increase in electrical efficiency and output power, respectively. Bayrak et al. [10] carried out experimental research on various cooling methods, such as PCM, thermoelectric, and aluminum finned heat sinks. The PV module combined with the finned heat sink generated the most power (47.88 W) compared to other cooling approaches. Passive approaches are also remarkably suitable for cooling PV systems when compared to active ones. The main benefit of passive cooling approaches is that the cooling system does not require an electrical input to work. As a consequence, the system is simple, with relatively low operational expenses. Amr et al. [11] investigated a passively cooled PV panel with fins affixed to the back surface of the module. The temperature of the cells has been decreased by about 4-5 ^{o}C by the integrated fins. Also, the electrical productivity of a PV system with fins is remarkably improved by increasing the height and number of fins.

Idoko et al. [12] investigated the tri passive cooling strategy, which includes three kinds: conductive, air, and water cooling. The experiment resulted in a 20.96 W increase in output power and up to a 3% improvement in efficiency, allowing the PV module to be more productive and cost-effective. Hernandez-Perez et al. [13] explored a new passive cooling method for solar panels, utilizing a segmented aluminium sheet connected to the PV module to reduce operating temperature and avoid a loss in electrical efficiency in adverse conditions. They were able to reduce module temperature by 9.40 °C while increasing module efficiency by up to 4%.

A novel PCM-based water-cooler nano-enhanced PCM system for passive natural cooling for the PV module has been tested by Abdollahi and Rahimi [14]. Experiments revealed that connecting nano-enhanced PCM to the PV module resulted in a 44.74% - 48.23% improvement in maximum output power relative to the reference module at solar irradiances of 410 W/m^2 and 690 W/m^2. Caglar et al. [15] tested experimentally an innovative photovoltaic thermal air (PVTa) system using quasi fins with a longitudinal and wavy profile at the tail end of the air channel for its

capabilities for hydrogen production. It was discovered that downstream-located fins improved PV panel cooling, increasing the current supply from the electrolyzer unit.

Floating photovoltaic systems (FPV) are another technique to improve the productivity of photovoltaic systems that have shown a lot of promise since 2006, with even greater ambitions for the future. Floating photovoltaic refers to PV systems that are mounted to floating platforms over accessible water bodies such as rivers, pools, or lakes [16]. FPV systems make it possible to achieve higher performance of PV modules and better land-resource management to ensure energy efficiency. It is an emerging topic for solar photovoltaic technology with a considerable worldwide market opportunity. Trapani and Millar [17] emphasized the importance of water bodies in cleaning the PV system and therefore enhancing performance. Cazzaniga et al. [18] demonstrated that the floating Photovoltaic system offers several benefits over the typical land-mounted system. They found that the temperature of the offshore ambient air above the water surface is up to 3°C lower than the temperature of the onshore air, resulting in a lower PV module working temperature. Moreover, the difference could be larger for more urban locations [19]. According to Choi [20], floating photovoltaic system outperformed terrestrial PV system in terms of efficiency by 11%. The deployment of PV systems on the water body, according to Tsoutsos et al. [21], reduces water evaporation. As proposed by Ates et al. [22], an FPV plant with a capacity of 2.03 GWp was anticipated to be deployed in Demirköprü Dam in Manisa, Turkey, on a surface area of 1,562.45 ha. . The deployment of such a system would produce 3.32 TWh of clean electricity yearly, preventing around 28.23×10^{6} m^3 of water from evaporating. Mittal et al. [23] used the RET Screen Expert software to investigate the feasibility of the FPV system in power production and water evaporation reduction in four lakes in Rajasthan, India, where the FPV system covered 5 to 20% of the lake's surface area. A 20% coverage FPV system might be adequate to construct a 27MWp plant, saving 708 million litres of water from evaporation yearly. Furthermore, the potential of the FPV system has been reinforced according to a comprehensive study done by Liu et al. [24]. The capacity of the FPV system in China is expected to reach 160 GW covering 2500 km^2 of water surface. This would assist to avoid the evaporation of 2×10^{27} m^3 of water each year. If conserved water could be utilized by hydropower, roughly 1.25×10^{12} m^3 of indirect water conservation would be further preserved. In Mumcular Dam, Turkey, the potential of an FPV system integrated with hydrogen production as a sustainable energy supply was investigated [25]. The proposed system has the ability to reduce evaporation from water bodies due to a 3010 m^2 shading area that provides

99.43% of the electricity needs. Muhammad et al. [26] looked into the feasibility of deploying FPV technology in Pakistan. Based on a comprehensive analysis of environmental, economic, and technological aspects, the adoption of such technology for Pakistan and other locations with comparable regional characteristics was justified and strengthened. Hasan and Dincer [27] utilized COMSOL software to evaluate the performance of a floating bifacial PV module compared to that of a mono-facial PV module under different working conditions. The simulation concluded that the bifacial module facing north to south witnessed a 55% higher irradiation exposure, while the deployment in wavy water simulation led to a 49 % increase in irradiation exposure. From April 2017 to March 2020, comprehensive research was conducted to analyze the performance of FPV systems using statistical methods, based on data gathered from the world's largest FPV testbeds, which were located on Singapore's Tengeh reservoir [28]. The results indicated that performance deterioration rates varied between -0.5% and -0.7% per year, which was inconsistent with the performance warranties provided by PV module manufacturers.

El Hammoumi et al. [29] conduct an experimental examination of a small-scale floating photovoltaic system (FPVS). Their findings revealed that the working temperature of the FPV system was 2.74 °C lower than that of the terrestrial PV system. Furthermore, up to 2.33%, more daily electricity is produced by the FPVS system than the terrestrial PV system. Dai et al. [30] had studied various designs and constructions of floating photovoltaic systems suitable for the deployment of floating farms at optimal performance. Kaymak and Şahin [31] investigated three distinct floating PV systems placed on Istanbul's Büyükçekmece lake, analyzing the obstacles and significant defects that might develop with such systems. Based on data collected between July 2018 and April 2020, it was strongly recommended that floating photovoltaics be designed as a whole to be flexible, and individual components must stay stable to withstand extreme wave and wind conditions. Cazzaniga et al. [32] proposed the idea of the pontoons that carry the floating PV system as reservoirs of compressed air for energy storage purposes with a high storage system. The behavior of a horizontal submerged photovoltaic solar panel in a water pool under a depth from 4 to 40 cm is explored by Rosa-Clot et al. [33]. In comparison to a conventional land-mounted PV module, the results showed an improvement in electric power production for shallow depths. Goswami et al. [34] performed a techno-economic study on a 10 MW floating PV plant showing the economic and environmental benefits through the adoption of FPV technology The outcomes revealed a 10.2% increase in power generation in FPV power plants compared to land-based PV systems, providing an extra 28.38 MU during the life span of the facility. Gonzalez

Sanchez et al. [35] explored the feasibility of FPV installation on accessible hydropower reservoirs in Africa. According to the findings, the installed capacity of existing hydroelectric power facilities can be doubled with less than 1% FPV coverage, while electrical production is increased by 58%. This would save water at 743 million m^3/year, which will increase annually the hydroelectricity of hydropower by 170.64 GWh. Kumar et al. [36] performed an exergy comparison between the three potential installation methods floating, submerged and land-mounted systems. The exergy efficiency of a submerged PV system is found to be 3.07% greater than that of a floating PV system and 43.65% higher than that of land mounted installation technique. Lanzafame et. al. [37] found out that an improvement in efficiency from 10 to 20% was reached for submerged PV in shallow water. Nevertheless, the above technique significantly depends on time and the location of the PV installation.

While floating photovoltaic plant technology is widely recognized, the Huainan project in China marks a major leap forward in the massive power capacity scale 40 MW, Fig. 1. The previous biggest floating photovoltaic system was a 6.3 MW project in the United Kingdom.

Fig. 1 The largest floating photovoltaic plant 40MW at Huainan, China [38].

According to the previous literature, the majority of the research studies were conducted on land-based PV modules that were integrated with a variety of active or passive cooling systems. Some of these studies were carried out experimentally in actual outdoor environments, while others were handled theoretically with the use of computer software simulation for productivity enhancement. Floating PV systems, on the other hand, have recently gained popularity, as the

installation of PV systems over water bodies has been demonstrated to enhance system productivity due to the cooler surrounding environment and reduced water evaporation.

The Novelty of the current work:

It is clear from this literature that much research has been conducted in the area of land-based PV systems. Some are based on an experimental method, while others are based on software package simulation. Nevertheless, based on the in-depth knowledge of these approaches, it is evident that there has been little experimental study done to investigate the performance enhancement of the floating photovoltaic systems. Furthermore, none of the prior studies examined passive cooling strategies to regulate the working temperature of the FPV system and consequently enhance its productivity. Finally, no previous research exists to investigate the performance enhancement of FPV systems on calm natural water surfaces, particularly in Egypt's hot climate, which is recognized for its high steady solar radiation, clear sky, and many extended lakes with calm water surfaces. The authors intended in this study to fill the resulting gap.

The present study is the first to employ a novel passive cooling approach for the FPV system. The proposed approach considers the partially submerged floating photovoltaic system PSFPV in the water body. The PSFPV system is a floating PV system deployed under Egyptian hot climate on calm water surfaces where a portion of the PV module is immersed in water to release some of the excess thermal energy into the surrounding water body including several lakes across Egypt, some of which are up to 5000 km^2 in area, such as Nasser Lake in Upper Egypt, all with the calm water surface, which acts as a natural costless heat sink. Fig. 2 depicts an outline of the suggested PSFPV system together with its objectives. The proposed investigation aims to study experimentally the performance of the PSFPV for various submerged ratios (β) which is the length of immersed portion /length of PV module. A comparison of the PSFPV system and a similar LPV system is carried out explicitly in terms of electricity productivity along with the thermal, economic, and environmental performances to assess the benefits of the PSFPV system.

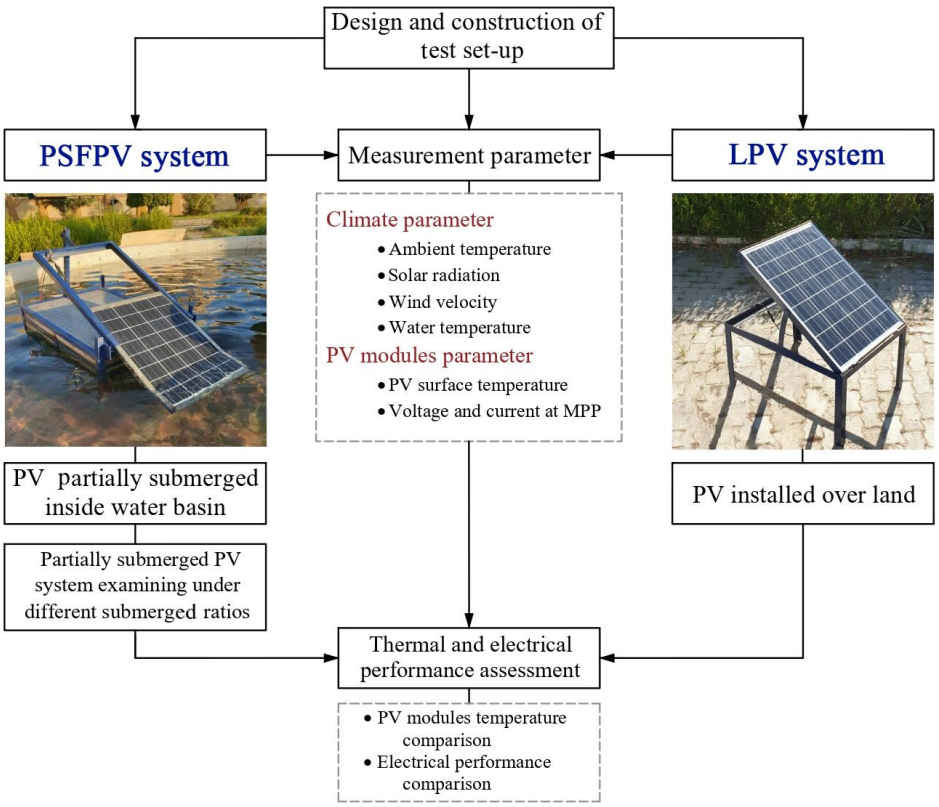

Fig. 2. Tests outline of the suggested PSFPV system.

2. Experimental setup

The experiments took place in June 2021 at the Faculty of Engineering (31°16´N, 32°18´E) in Port Said, Egypt. For the current work, two photovoltaic modules (PV) were used, one placed inside a water basin of a five-meter radius for simulating a water body while the other module was mounted on the ground. Panels were orientated to the south due to Egypt's location in the northern hemisphere. The entire PSFPV system was anchored with a mooring mechanism to retain the specified orientation. Both panels were installed next to each other in the same outdoor conditions and tilted with a control mechanism at an angle (θ=25º) to the horizontal plane for optimum solar radiation. A sliding frame with a holder was employed to facilitate our investigation about the effect of the submerged segment length of the PV panel in the water as seen in Figs. 3, 4.

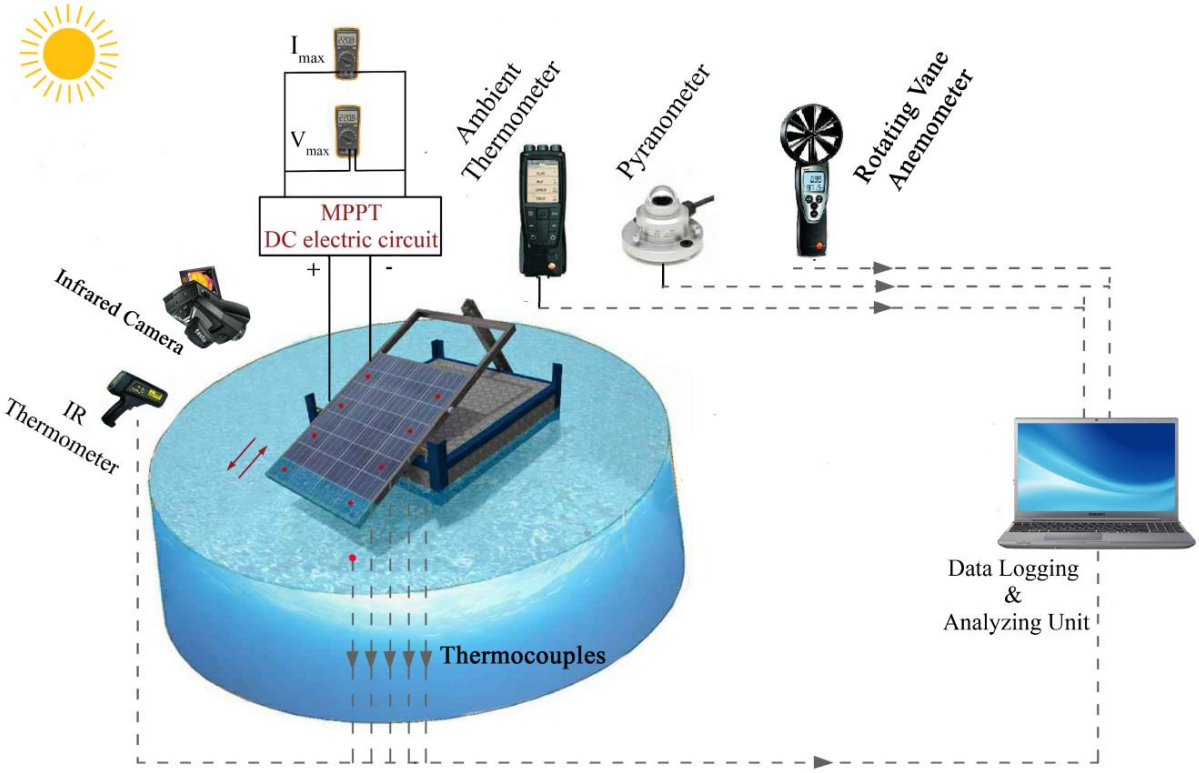

Fig. 3. Experimental setup

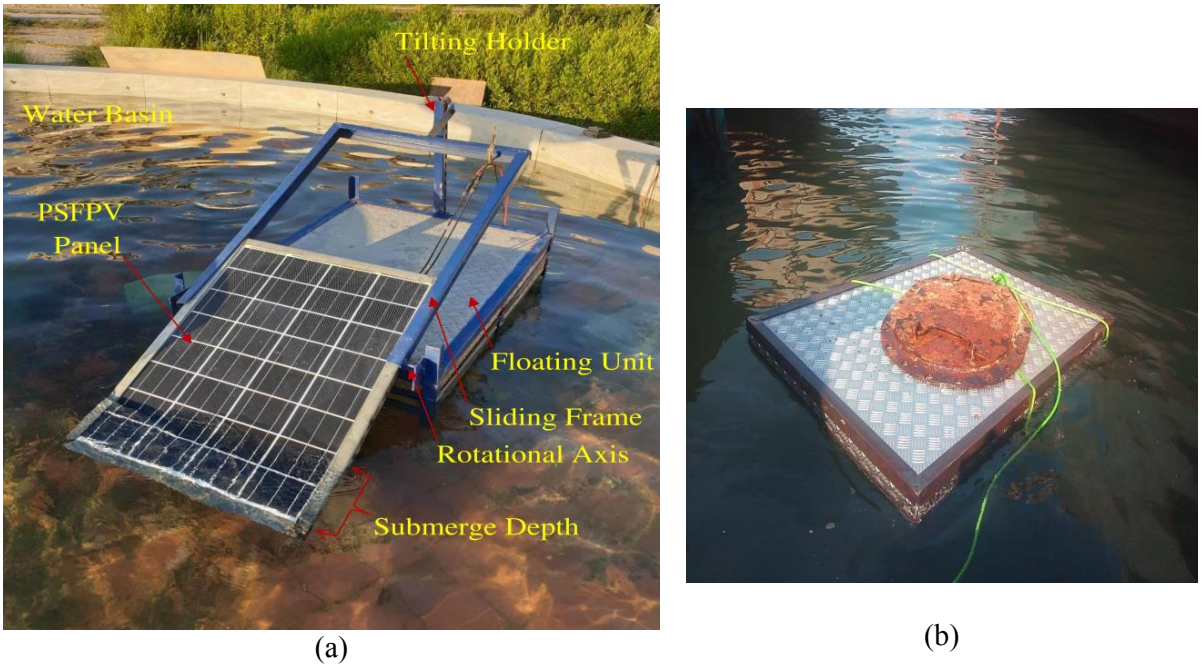

(a) (b)

Fig. 4. (a) Photograph of the PSFPV system, (b) stability testing of the floating unit in open sea.

The experiment setup was performed using two identical PV modules with a capacity of 83 W each. The PV solar panel specifications are listed in Table 1.

Table 1

brand	S-ENERGY
Panel type	Polycrystalline
Dimensions in mm	920 × 680 × 38
[I_{sc}] (A)	5.78
[V_{oc}] (Voltage)	19.7
[$P_{m_{STC}}$] (W)	83
[V_{mp}] (Voltage)	16.5
[I_{pm}] (A)	5.07
[Pmax] NOCT* (W)	60

NOCT*: Nominal Operating Cell Temperature: 47℃

Several measuring instruments were used throughout the experiments, from 08:00 a.m. to 06:00 p.m., to assess the influence of the variable under consideration on the overall performance of the PV system. Table 2 depicts the main measurement instruments used in the experimental setup, their accuracy, and range.

Experimental measures were captured at intervals of 30 min each day by recording the measured parameter through the various devices mentioned. The solar irradiance received by both LPV and PSFPV surfaces was captured by Hukseflux SR20, an A-class pyranometer with a sensitivity range of 7 to 25 × 10^{-6} V/(W/m^2). Nemours pre-calibrated type T thermocouples along with an Infrared thermometer have been employed to detect the surface temperature of both systems in various positions along with the temperature of the submerged segment of the PSFPV module, to measure the average operating surface temperature of both panels. Another thermocouple monitored the bulk temperature of the water basin in which the PSFPV was submerged. Ambient temperature has been measured using a digital thermometer Testo 480 when the wind velocity has been captured by rotating vane anemometer Testo 417.

The average operating temperature T_{av} of the PV modules was calculated according to the following equation:

$$T_{av} = \frac{\sum_{i=1}^{n} T_i}{n} \quad (1)$$

Thermal contours for the front surface of the PSFPV module were captured using an infrared thermal camera (model testo 890) with a measurement range of -30 to 650°C. The emissivity of the inspected thermal seine was set at 0.94 for the glass as the front layer of the PV module [39]. The thermal images are captured from a constant distance by pointing the camera lens in a perpendicular direction with the module instantaneously removed from the water body for emissivity equality.

Table 2

Experimental apparatuses with their range and accuracy.

Apparatus	type	Accuracy	Range
Pyranometer	Hukse flux SR 20	> ±1.2%	0 to 4000 W/m^2
Voltmeter	Fluke 175 True RMS	± 0.15%+2	0.01mV to 1000DCV
Ammeter	Fluke 175 True RMS	± 1.0%+3	0.01 mA to 10 DCA
Thermocouple	T-type	± 0.05 ºC	- 250ºC to 350 ºC
Infrared thermometer	Spot type	±0.3 °C	-50 to 600 °C
Atmospheric thermometer	Testo 480	± 0.3 °C	0 to 120 °C
Infrared thermal camera	Testo 890	±2%	-30 to 650°C
Rotating vane anemometer	Testo 417	± 0.1 m/s	0-20 m/s
Data acquisition	Midi LOGGER GL840	± 0.1%	--

The maximum electrical output power P_m in W was obtained by wiring the electrical outputs of both modules to the adjustable electric resistance circuit and recording the I-V curve for each system on a half-hourly basis. The voltage and current values obtained using digital multi-meters (Fluke 175 True RMS) are then analysed in way to construct the characteristic curve between voltages and currents and identify the maximum power point MPP [40,41]. The electrical efficiency η_{elec} of both modules were then calculated with the following formulas:

$$P_m = V_m \times I_m \tag{2}$$

$$\eta_{elec} = \frac{P_m}{GA_s} \times 100 \quad \% \tag{3}$$

where G is the irradiation gauged in W/m^2, and A_s is the active solar harvesting area of the panel in m^2.

The normalized power output efficiency NPE is another parameter that reflects the true performance concerning the tested conditions [42]. The NPE computed using Eq. (4), is the ratio

of power recorded under real conditions to output power measured under the standard conditions ($P_{m_{STC}}$), as read from the panel's nameplate.

$$NPE = \frac{P_m}{P_{m_{STC}}} \times 100 \qquad (4)$$

The performance ratio PR is one of the most important indicators for assessing the efficiency of the photovoltaic systems and for evaluating various sites for PV installations independently of solar irradiation, as seen in Eq. (5). It is a parameter with no units that reflects the influence of irradiance on the output of the PV module.

$$PR = \frac{P_m / P_{m_{STC}}}{G / 1000} \qquad (5)$$

The uncertainty of the instruments during the experimental measurements was examined to assess the precision of the experimental data, which may have been affected by possible errors in the parameter measurement tests [43–45]. The uncertainties in the independent variables via the evaluation procedure are denoted as W_1, W_2, ……and W_n, with the uncertainty in the result W_R being obtained from the following equation, where x_1, x_2, …, x_n, are the independent variables.

$$W_R = \left[\left(\frac{\partial R}{\partial x_1} W_1 \right)^2 + \left(\frac{\partial R}{\partial x_2} W_2 \right)^2 + ... + \left(\frac{\partial R}{\partial x_n} W_n \right)^2 \right]^{\frac{1}{2}} \qquad (6)$$

According to eq. (6) The maximum calculated uncertainty for the electrical efficiency was evaluated as following

$$\eta_{elec} = f\left(I_m, V_m, G\right) \Rightarrow W_{\eta_{elec}} = \left(\left(\frac{\delta \eta_{elec}}{\delta I_m} W_{I_m} \right)^2 + \left(\frac{\delta \eta_{elec}}{\delta V_m} W_{V_m} \right)^2 + \left(\frac{\delta \eta_{elec}}{\delta G_m} W_G \right)^2 \right)^{\frac{1}{2}} = \pm 0.2 \qquad (7)$$

Similarly, the maximum uncertainty for PR was ± 0.012. The maximum uncertainties of variables were found to be less than 5%, which revealed a high accuracy in measurements.

3. Results and discussion

The experiments were conducted under typical metrological conditions to explore the effect of submerged ratio β on the overall performance of the PSFPV system for six test days, from the 10th to the 16th of June 2021, and compare it with the LPV system

The thermal and electrical behaviour of PSFPV system were extensively examined for submerged ratios of 4%, 12%, and 24%, and compared to those of LPV system, as shown in Fig. 5. Throughout the experiments, solar irradiance, atmospheric and water temperature, and wind velocity were recorded as a sample of the climate parameters that vary during the test days, Fig. 6.

(a) β = 4% (b) β =12 %

(c) β = 24%

Fig. 5. Photographs of the examined submerged ratios of the PSFPV system.

The solar intensity peak reported over the test days was about 1020 W/m^2, as shown in Fig. 6. Furthermore, a little fluctuation in average solar radiation and ambient temperature was observed for the experimental test days. In addition, during the test days, the water temperature increased at

a relatively steady rate, reaching its maximum value towards sunset. Wind velocity has been captured to inventory the climatic parameter that influences the performance of the PV solar panel.

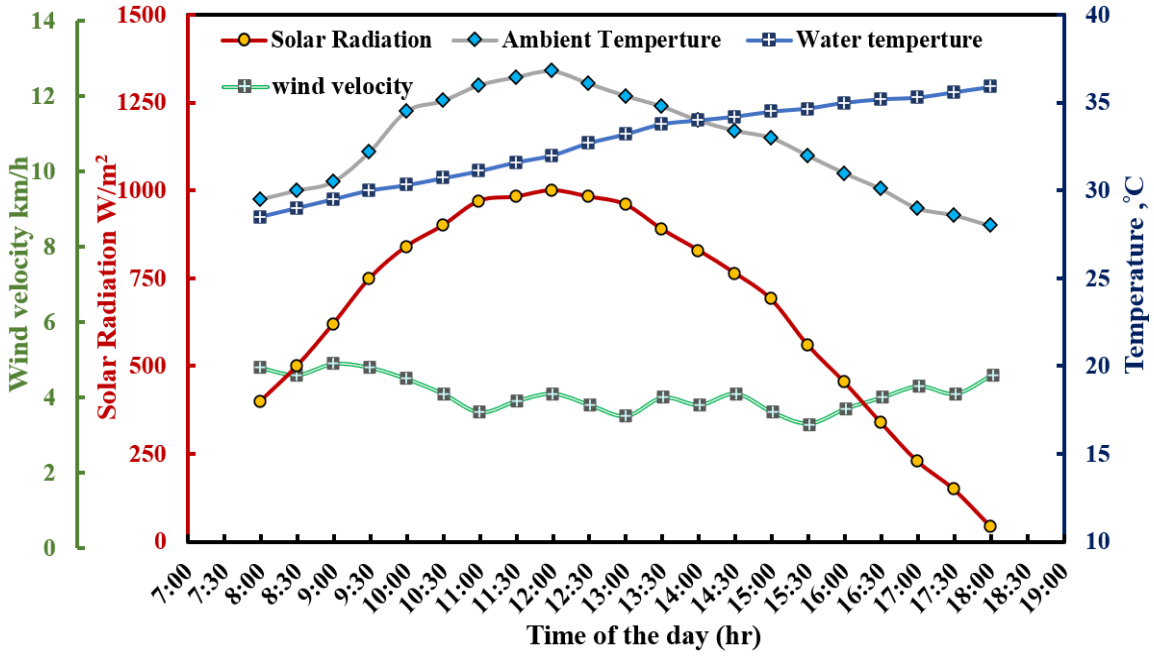

Fig. 6. Sample of the climate data recorded during the experiment.

3.1 The influence of submerged ratio on the working temperature of the PV module.

The influence of the submerged ratio on the performance of the PSFPV system is mostly reflected in the module temperature. Fig. 7 presents the working temperatures of the PSFPV module with the studied submerged ratios, i.e., 4%, 12%, and 24%, along with those temperatures of the land based LPV module. In this set of experiments, the tilt angles of both modules were fixed at 25°. It can be noticed that the working temperatures of PSFPV for all tested submerged ratios were reduced as compared to the reference LPV module.

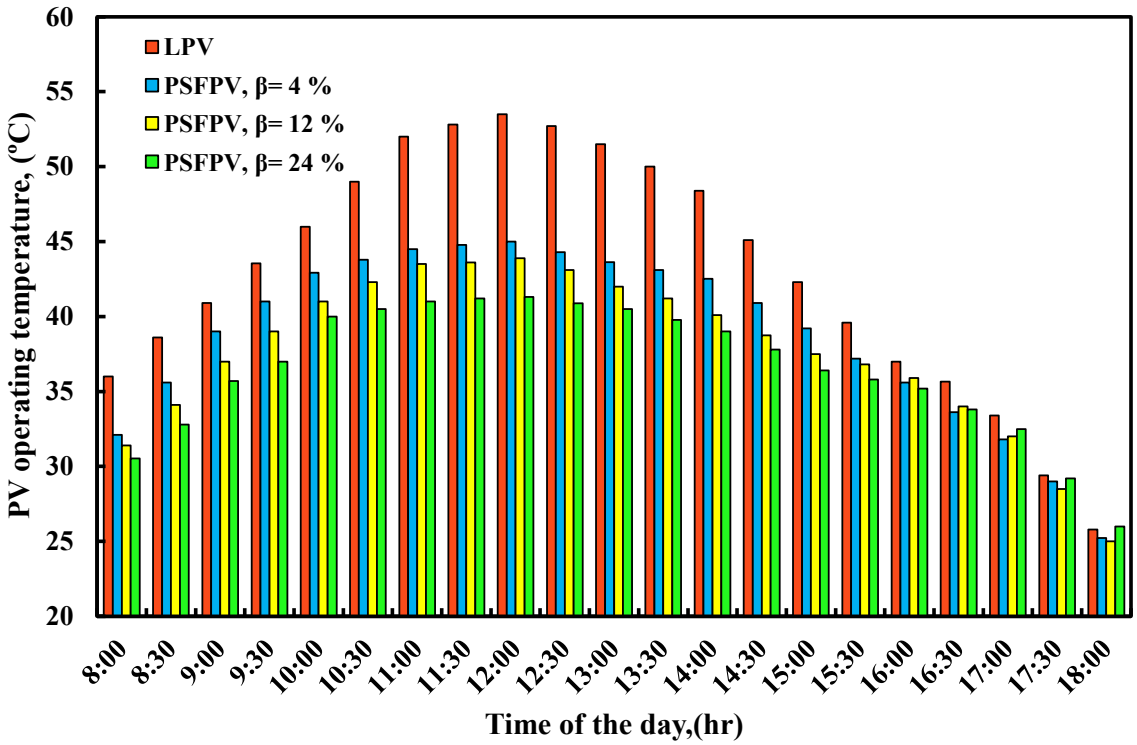

Fig. 7. PV operating temperature for the examined submerged ratios.

The operating temperature of the PSFPV panel was noticeably reduced when the submerged ratio was increased. The average operating temperatures of the PSFPV panel for the tested submerged ratio, i.e., 4%, 12%, and 24%, were 38.80 °C, 37.65 °C, and 36.52 °C, respectively, compared to 43.01 °C for the LPV panel. This plot also demonstrates that the maximum operating temperature differences between PSFPV and LPV modules were 8.50 °C for β =4%, 9.60 °C for β=12%, and 12.20 °C for β=24% at noontime.

Thermal profiles of both the LPV and the PSFPV modules with the examined submerged ratios were captured using an infrared thermal camera (model testo 890) while conducting the tests at noon, as shown in Fig. 8. The colour patterns across the surface of the PSFPV module show an improvement in lowering the operating temperature. The thermal profile is coloured from red to blue, as seen in the thermal images below. The reddish tint denotes a relatively high operating surface temperature, whereas the blue tint denotes a low working surface temperature. As seen in Fig.8, the reddish spot's range practically spans the whole surface of the LPV module. However, for the PSFPV module, the range of the reddish spot steadily vanishes as the submerged ratio increases. Furthermore, the thermal pattern of the PSFPV module's immersed section inside

the water is shown to have remained at a markedly decreased temperature, as indicated by the blue colouring. This occurrence reveals that, as a result of the recently implemented immersion approach, the operational temperatures of the PSFPV system have been substantially lowered.

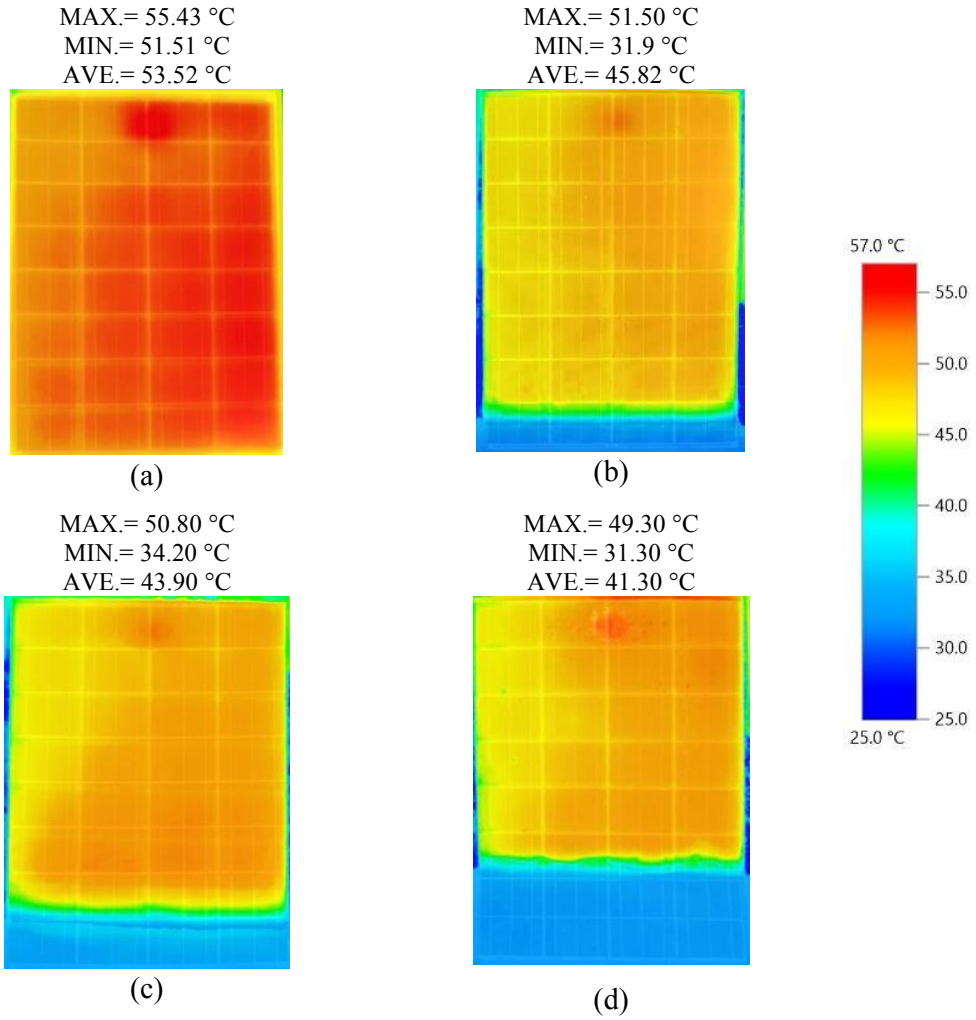

Fig. 8. Thermal profile for: (a) LPV compared to PSFPVs modules at the submerged ratios; (b) β = 4%, (c) β= 12%, and (d) β = 24% at noon.

3.2 The effect of submerged ratio on the electrical behaviour of the PV module

The electrical productivity of the PV system is the most crucial parameter to focus on in this study, as this is high-grade energy. The electrical performance might be determined by measuring the loaded voltage and current, and also the electrical power output. Fig. 9 demonstrates the variation of the current flowing through the electrical circuit for all the submerged ratios studied, whereas Fig. 10 presents the voltage readings of the PV module for all the submerged ratios studied

throughout the day. The findings indicate that voltage and current follow the solar radiation pattern, increasing from dawn to the solar peak time, which is between 11:00 a.m. and 1:00 p.m., and then decreasing till sunset. It can be seen that the current and voltage have been predominated for all of the PSFPV modules from the morning until 03:00 p.m.

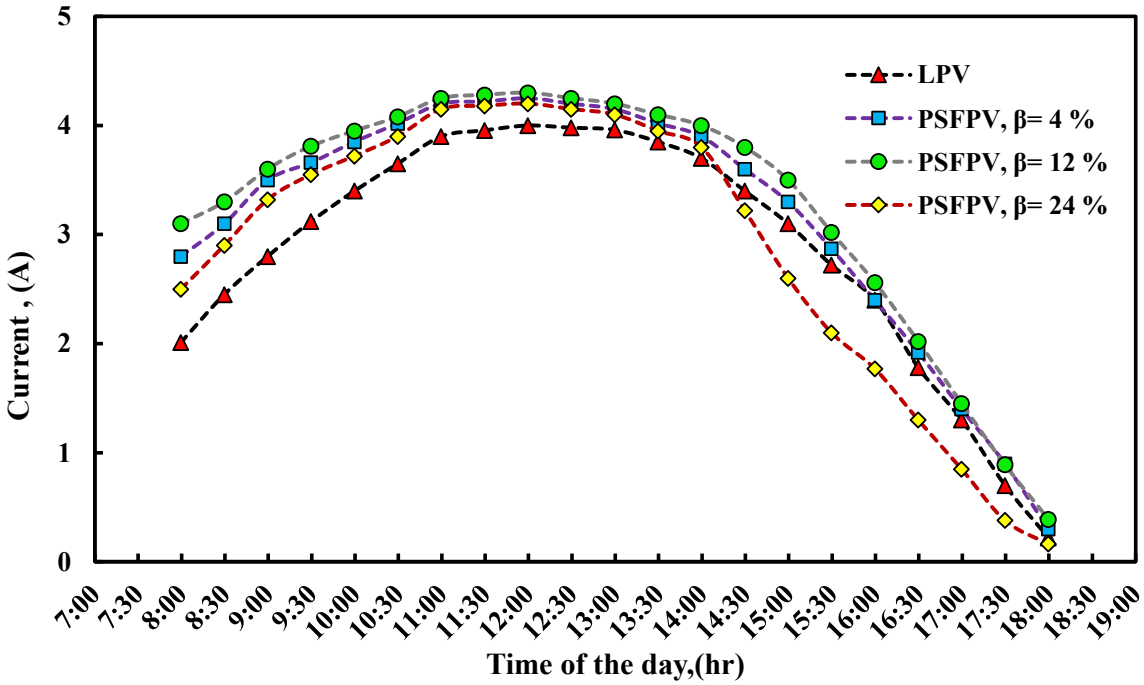

Fig. 9. Current variations of the PV module for the examined submerged ratios.

The maximum measured voltages for the PSFPV system are 15.24 V, 15.37 V, and 15.01 V for submerged ratios of 4%, 12%, and 24%, respectively. For the LPV system, the maximum recorded voltage is 14.61 V.

Similarly, the recorded daily averaged voltages of the PSFPV module were about 12.46 V, 12.84 V, and 12.01 V for the submerged ratios of 4%, 12%, and 24%, respectively, and the daily averaged voltage for the LPV system is 12.08 V.

Moreover, the average daily currents of the PSFPV module were 3.17 A, 3.28 A, and 2.90 A for the submerged ratios of 4%, 12%, and 24%, respectively while the averaged current of the LPV system was 2.88 A.

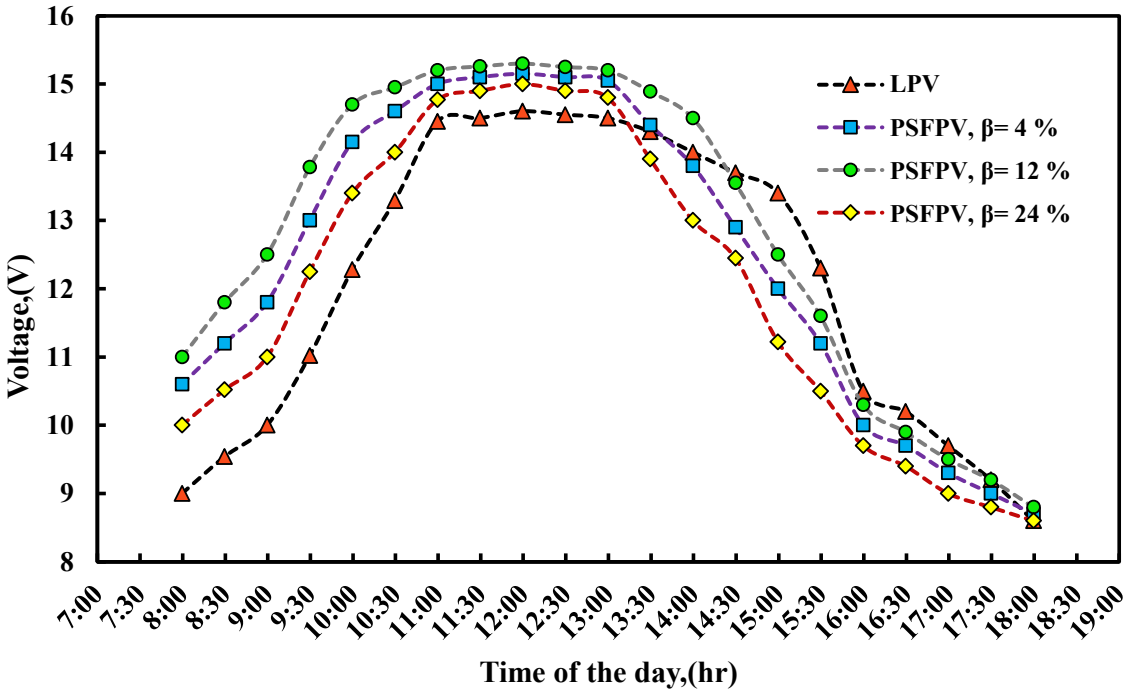

Fig. 10. Voltage variations of the PV module for the examined submerged ratios.

The recorded values of the power output of the PSFPV system for the examined submerged ratios, along with those values of the LPV system are shown in Fig. 11. Output power superiority was observed for the PSFPV module, as evidenced by the voltage results, with all submerged ratios tested till 03:00 p.m. Also, the maximum outputs of 64.39 W, 65.79 W, and 63.00 W were reported at midday at submerged ratios of 4%, 12%, and 24%, respectively. The daily average output power of the PSFPV system was 41.89 W, 44.53 W, and 37.45 W for the submerged ratios of 4%, 12%, and 24%, respectively. Meanwhile, the daily average output power of the LPV panel was 36.87 W, with a peak of 58.40 W at noon. A power enhancement of 17.44% and 27.31% has been achieved in the PSFPV module by increasing the submerged ratio from 4% to 12% respectively.

It was observed that the PSFPV module with a submerged ratio of 10% achieved the highest power generation over the other studied ratios. The justification for this is that raising the submerged ratio lowers the PSFPV operating surface temperature, which could, in turn, enhance the module's productivity.

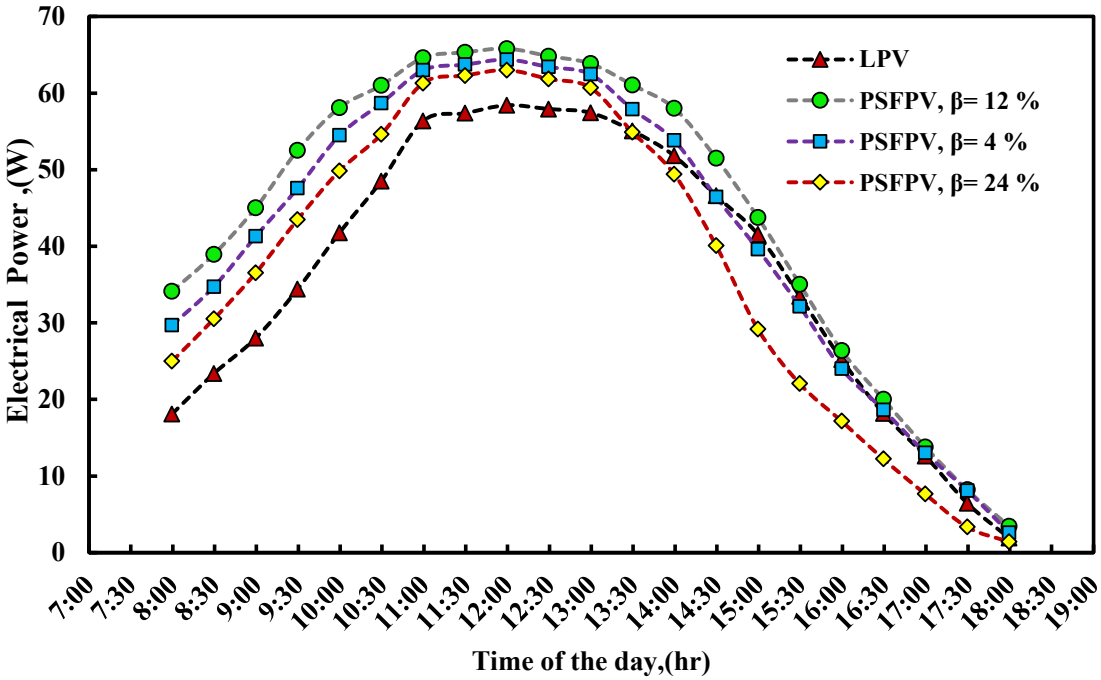

Fig. 11. Electrical output for the PV panel for the examined submerged ratios.

As previously mentioned, the PSFPV module dissipates more excess thermal energy; however, once the solar radiation hits the water's surface, a small portion of it is reflected, dispersed, and even absorbed by the aqueous medium according to irradiance characteristics [32]. The remaining radiation would be transmitted through the water until it hit the underwater part of the PSFPV panel. However, by increasing the submerged segment of the PSFPV panel, a small amount of the solar irradiance would be distorted and hindered from reaching the submerged part. The drop in the temperature of the PV panel pays off for the diffused radiation, and even boosts the panel's performance, as spotted in the experimental results.

The effect of the submerged ratio on the PSFPV module's efficiency was investigated and compared with the equivalent LPV module. Fig. 12 demonstrates the electrical efficiency variation of the PSFPV module at the examined submerged ratios, 4%, 12%, and 24% respectively. The reported data showed that the PSFPV module outperformed the LPV module almost throughout the day, with the exception of the last two hours, as noted. The daily averaged electrical efficiencies of the PSFPV module for the three submerged ratios ranging from 4% to 24% were 12.08%, 13.24%, and 10.58%, respectively, whereas the LPV's averaged efficiency was 10.73%. It was also concluded that the PSFPV module with a submerged ratio of 12% attained the highest

efficiency, and therefore the best performance since it balanced between the boost from the cooling effect and the minimum radiation losses.

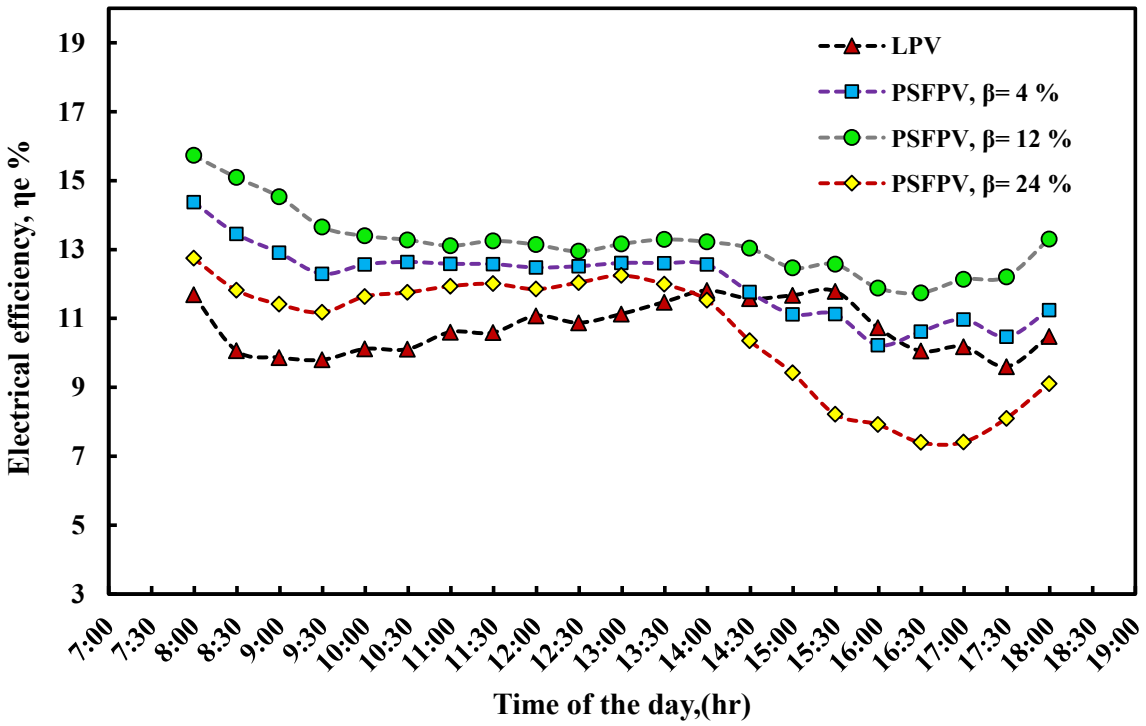

Fig. 12. Electrical efficiency for the PV module for the examined submerged ratios.

The average thermal and electrical performance of the examined PSFPV systems has been summarized in Fig. 13 and compare their performances with the conventional LPV system. The PSFPV with β=24% achieved the lowest operating temperature with a temperature reduction of 4.21℃relative to the LPV system. However, the PSFPV at =12% with less radiation diffusion has the best electrical performance. An absolute percentage error has been demonstrated in the Fig. 13 for every averaged value calculated.

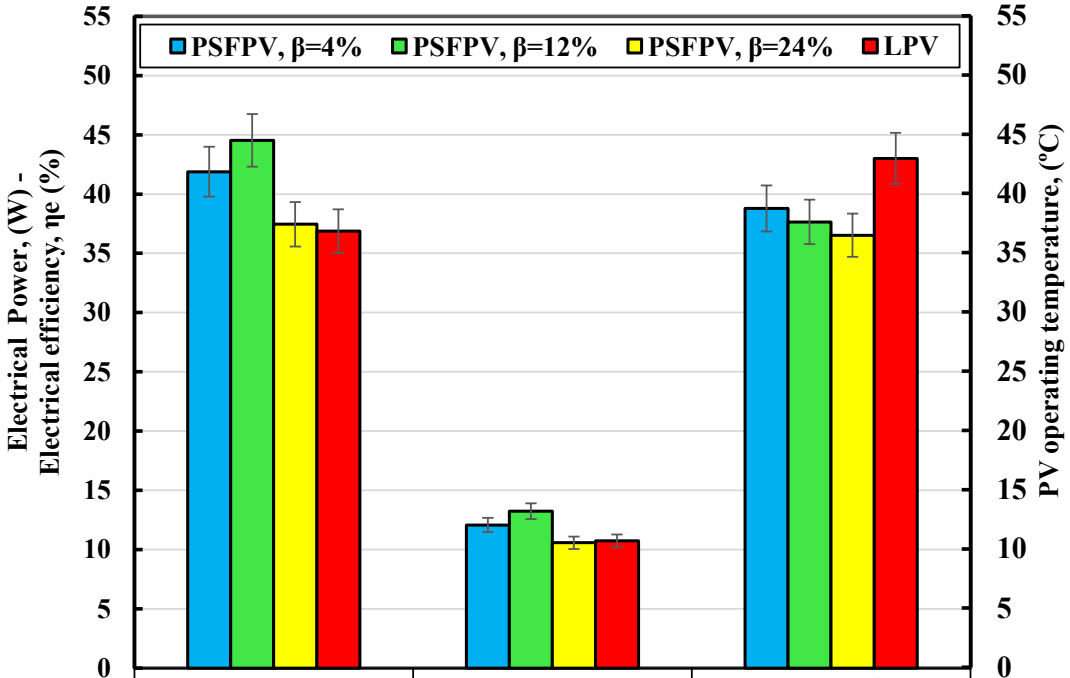

	Electrical Power, (W)	Electrical efficiency, ηe (%)	PV operating temperature, (°C)
PSFPV, β=4%	41.89	12.08	38.80
PSFPV, β=12%	44.53	13.24	37.65
PSFPV, β=24%	37.45	10.58	36.52
LPV	36.87	10.73	43.01

Fig. 13 Average thermal and electrical performance of the examined PSFPV systems.

The NPE was plotted against the solar irradiation as shown in Fig. 14. It was obvious that the PSFPV indicated superior performance compared to the LPV as the cooling effect started to pay off with increasing the solar radiation above 400W/m^2. At high solar radiation intensity, the PV operating temperature elevated which in turn has a negative effect on the productivity of the module. The submerged portion acts as a heat sink, realizing the excess heat in the lower part of the module into the water body as presented in Fig.14.

The performance ratios (PR) were determined and averaged according to eq. (5) for both PSFPV and LPV modules. Fig. 15 illustrates the PR values, solar radiation during the hours of 8:00 a.m. to 06:00 p.m. for all the examined submerged ratios of the PSFPV module along with those values of the LPV module. The daily mean PR was enhanced from 0.75 to 0.82 with increasing the submerged ratio from 4% to 12%, whereas the daily average PR for the LPV system was 0.66. It

was concluded that an improvement of 12.60% to 23.00% for the submerged ratio from 4% to 12% was achieved when compared to the LPV module. It has been noticed that throughout the peak solar irradiance, the PR fell due to the elevated working temperature of the PV module during this period.

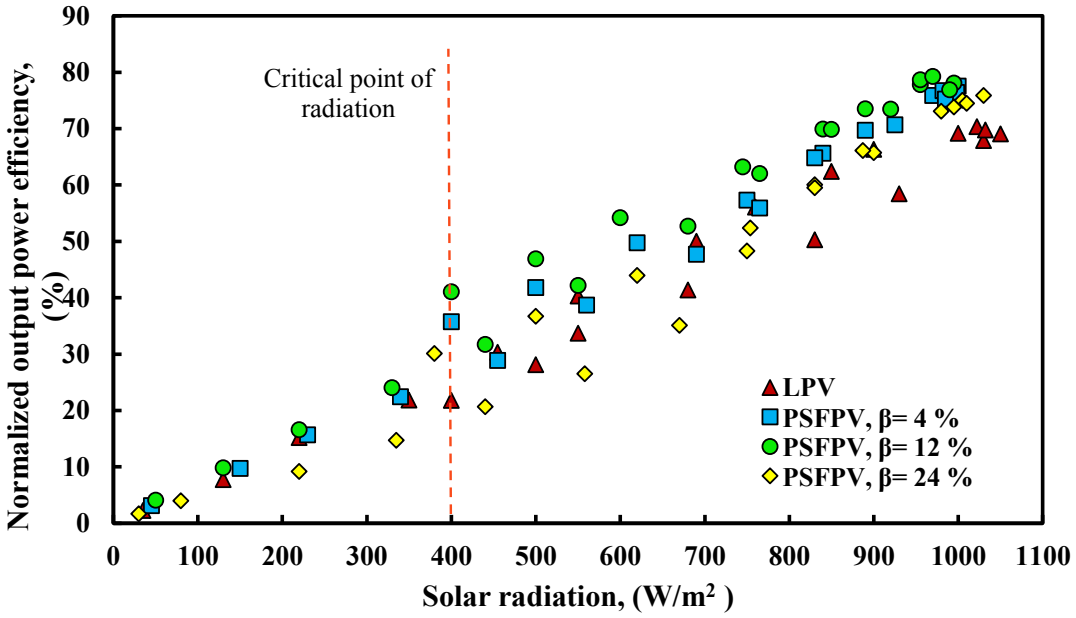

Fig. 14. Normalized power output efficiency for the PV module for the examined submerged ratios.

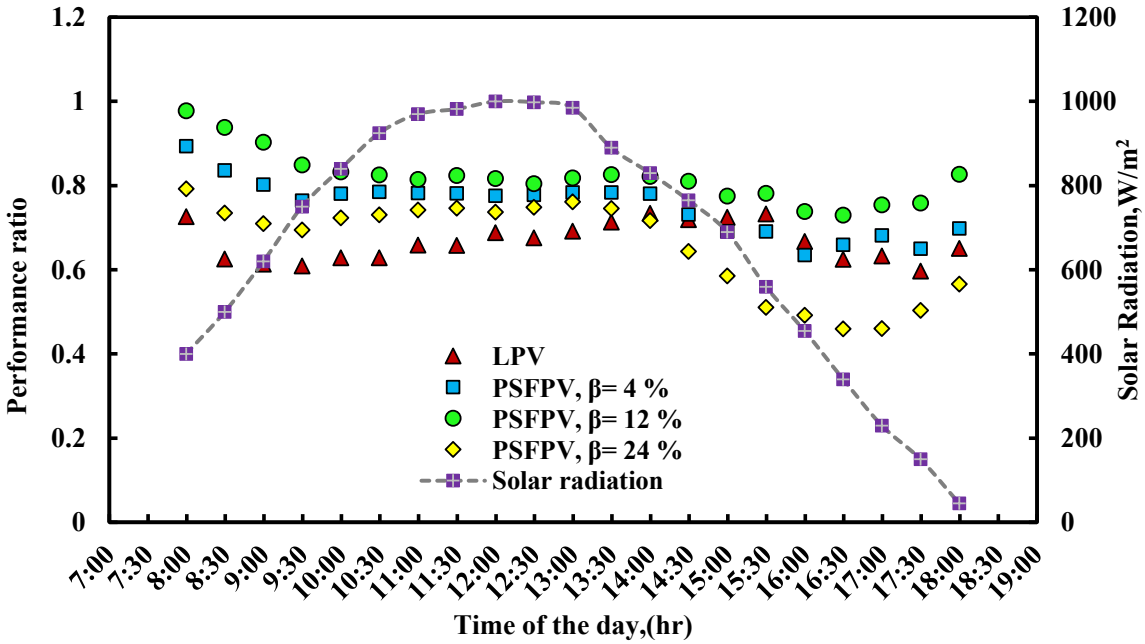

Fig. 15. Performance ratio and irradiance for the PV module for the examined submerged ratios.

A multi-factor analysis of variance (ANOVA) was used to test the effects of the submerged ratio on the electrical efficiency and the NPE thought out the day [46,47]. A polynomial regression model was developed using the experimental results from the NPE and the efficiency measured and calculated over the experimental test days. Equations (8,9) predict the instant NPE and efficiency of the PSFPV as a function of; t: time of the day in hr, β: submerged ratio, and G: solar intensity measured in W/m^2 for ambient temperature range of 30–36.8°C as the performance of the PSFPV were significantly affected by these variables throughout the day. The equations were based on the actual factor's values, which can be used to make predictions about the responses

$$NPE = 34.145 - 2.041t + 128.288\beta + 9.49 \times 10^{-3}G + 1.83 \times 10^{-3}\,tG - 553.674\beta^2 + 3.4 \times 10^{-5}G^2 \quad (8)$$

$$\eta_e = 88.911 - 14.258\,t + 32.908\beta - 8.1 \times 10^{-5}G + 1.162 \times 10^{-3}\,tG + 1.478 \times 10^{-2}\beta G + 0.549t^2 - 178.869\beta^2 \quad (9)$$

The plots in Figs. 16,17 present the predicted values against the experimental values, which demonstrate that the points close to the line indicate the similarity between the two values (experimental and predicted).

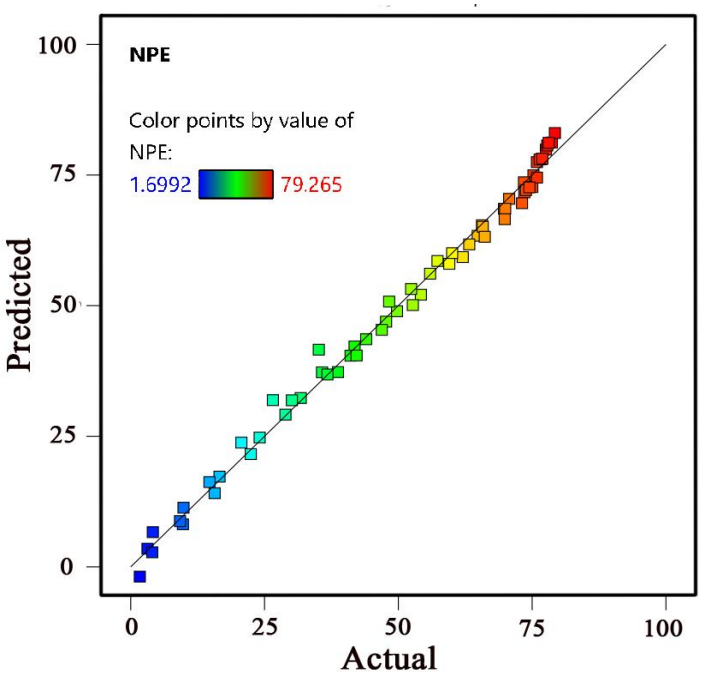

Fig. 16 Predictions of the calculated NPE against the experimental values.

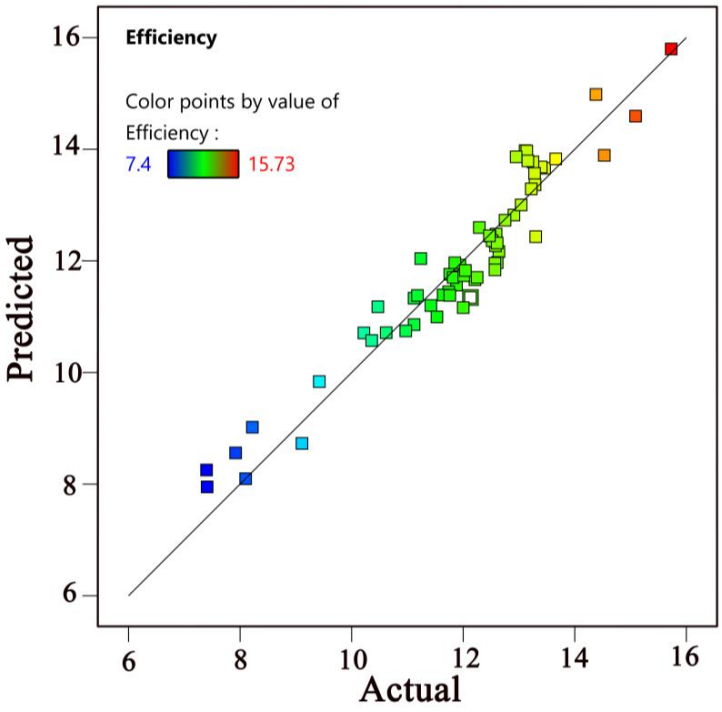

Fig. 17 Predictions of the calculated efficiency against the experimental values.

The 3D surface plot in Fig. 18 shows the impact of submerged ratio on the instant electrical efficiency throughout the day.

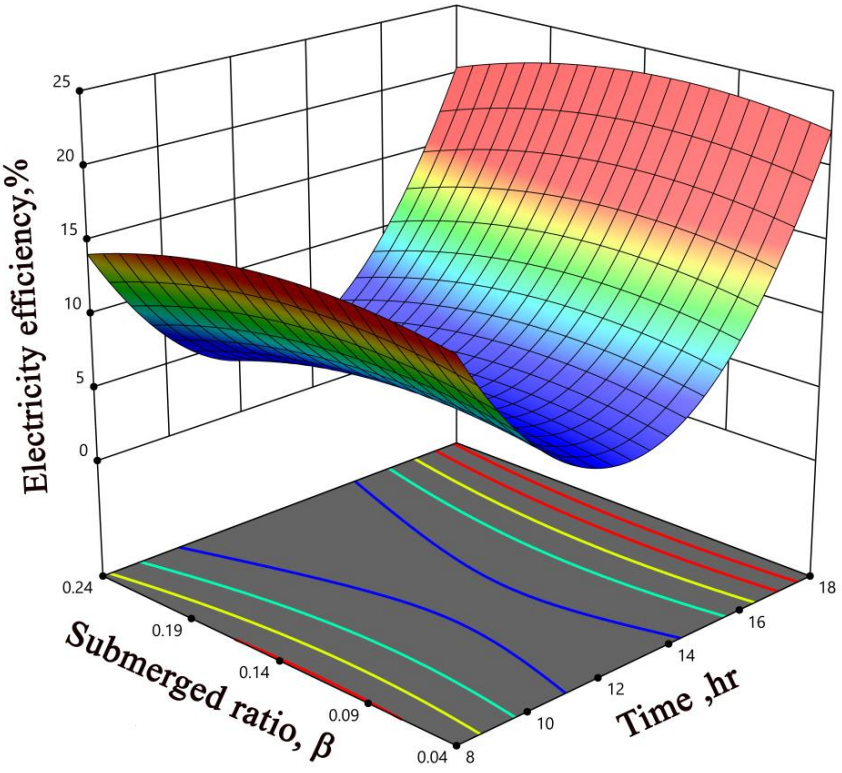

Fig. 18 A 3D surface graphic depicts the change in instantaneous electrical efficiency for a variety of submerged ratios.

1. **Carbon dioxide CO_2 emission reduction Environmental benefits**

The trend of decarbonizing electricity generation at the global level has been undertaken in order to decrease the pernicious effects of greenhouse gas emissions. Fossil fuel combustion is the primary source of CO_2 emissions, contributing to air pollution and environmental degradation. In addition, Egypt has a high potential for solar radiation, making it one of the best candidates for investment in solar energy and, at the same time assist in reducing CO_2 emissions. The proposed PSFPV system, which would use accessible lakes and water bodies, would save CO_2 emissions while improving system performance and reducing water evaporation as well as power

enhancement, enabling greater savings in terms of CO_2 emissions. The degree of CO_2 emissions reduction has been estimated the following formula:

$$CO_2 \text{ emissions savings from PV system per day} = CO_2 \text{ emissions intensity for electricity generation (g of } CO_2\text{/KWh)} \times \text{Energy generated (KWh/day)} \quad (10)$$

It has been found that, for coal-fired thermal power plants, the mean carbon dioxide (CO_2) emission rate for electricity generation is 890 (g/kWh) [48,49]. It should be noted that adopting the submersion technique for PSFPV systems leads to daily CO_2 emissions reductions of about 382.97 g, 405.83 g, and 340.83 g for submerged ratios of 4%, 12%, and 24%, respectively. The entire summer carbon dioxide mitigation is approximated using daily power output recorded throughout the experiments since the variance in Egypt's solar radiation is so small throughout the summer season (June to September). The plot in Fig. 19 reveals the power produced and its CO_2 emission saving potential from clean electricity production for various submerged ratios per summer season. In the case of the optimal condition at β= 12% and a tilt angle of 25º, the total reduction in CO_2 emissions was 49.66 kg of CO_2 per summer season.

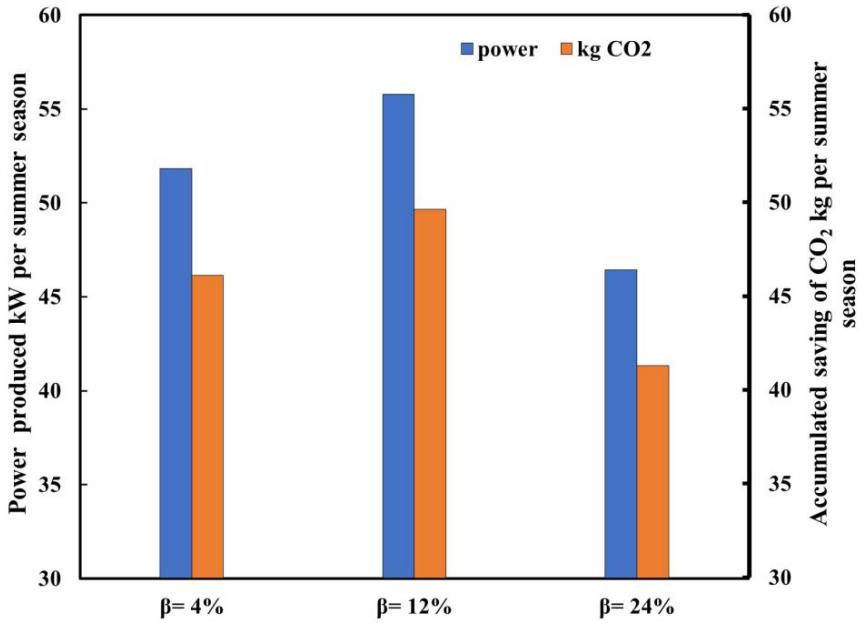

Fig. 19. The electrical power produced and saving in CO_2 for submerged ratios per summer season.

2. Economic estimation

The economic perspective is perhaps the most constraining factor before making the final decision. Researchers are trying to use techniques that not only provide significant heat transfer improvements for PV systems but also provide reasonable financial benefits. Inevitably, from an economic point of view, any enhancement approach should also be evaluated. The Levelized Cost of Electricity (LCOE) is a very well approach for quantifying the economic feasibility of the electric power produced from the cooled PSFPV which enables the costs assessment of the system over its lifetime T [50,51].

LCOE can represent the cost of the anticipated power produced by a certain system considering the total cost spent throughout its life span as expressed in eq. (11) [52–54].

$$LCOE = \sum_{t=0}^{T} \frac{IC_t + O_t + M_t}{(1-i)^t} \Big/ \sum_{t=0}^{T} \frac{E_o (1-d)^t}{(1-i)^t} \qquad (11)$$

Where IC_t is the capital investment costs includes the cost of the solar component and floating unit. Hence, Table 3 provides the following cost analysis based on the foregoing hypothesis.[55]. O_t and M_t are operation and maintenance costs of the system spent during the period t respectively. E_o is the expected annual rated energy output of the system during the first-year operation while d is the decay rate of the PV module (%) throughout the precise cycle due to semiconductor degradation, and connection ribbon and adhesion losses [56]. The balance of plant (BOP) expenses, embraces the costs coupled with the electrical circuit and protection equipment required. Considering that the service period of both PSFPV and LPV systems T is 25 years and the annual interest rate (i) was taken as 10% [57]. Solaris Synergy has been preferred as a float supplier due to its less complex structure, which can be easily produced with locally available materials [58].

Table 3

Cost breakdown of solar components for both PSFPV and LPV systems [59–61].

Components	USD/Wp
	PSFPV
PV module	0.22
BOP	0.23
Electrical components	0.1
Engineering, Procurement, and Construction (EPC)	0.31

The floating components [58].	
Floater supply	0.1
Moorings and anchors supply	0.04
Engineering, Procurement, and Construction (EPC)	0.1
Operation & maintenance cost (USD/Wp /year) [62].	0.026

The operation and maintenance costs have not been well documented for neither FPV nor PSFPV system. These expenses are yearly costs to sustain the plant's productivity, i.e. to optimize power output and the life span of the plant [63]. It is stated that the maintenance costs are limited for the floating system throughout the life cycle. In the cleaning process of floating PVs, the on-site availability of water can be a benefit, but the presence of mooring lines and anchors may also mean that the operation and maintenance costs may be high [64]. In LCOE analysis, the tax rate was not taken into consideration, which normally is different from region to region. It can be seen that the calculation of LCOE for the LCOE for the PSFPV system was slightly reduced from 0.075 to 0.067 ($/kWh) by increasing the submerged ratio from 4 % to 12 %; therefore, the relative LCOE was decreased by 7.52% due to the proposed cooling system. The proposed cooling mechanism has produced a higher PV efficiency and lower operating temperature for PV. A sensitivity analysis of the LCOE was explored by Barbuscia [65] confirmed that the system's installed capacity has an almost exponential declining pattern as installed power rises, approaching values close to those of traditional technology for utility-scale systems.

3. Conclusions

Designing and testing the floating photovoltaic system with various configurations have already been investigated by many researchers but, none of the previous research works studied the performance of the partially submerged PV system. In this article, the overall performance of the PSFPV system is experimentally explored for the first time.

- This cooling effect has been fully investigated and experimental results affirm the potentiality of acquiring up to 27.31% in electricity higher than the standalone PV without cooling.
- The study found that the temperature of the PSFPV module is always lower throughout the test period than that of the LPV module, with a difference of up to 12.20 ºC, the electrical efficiency of the PSFPV system can increase by about 23.57% compared with a standalone terrestrial PV system.

- The submerged ratio is found to be a highly effective parameter on the operating temperature and overall efficiency of the PSFPV system.
- The optimal value for submerged ratio (i.e., to minimize the operating temperature and maximize the overall efficiency of PSFPV is found to be 12%.
- Based on the normalized power output efficiency analysis, it was revealed that the critical point of radiation at which the cooling effect started to pay off with increasing the solar radiation was above 400 W/m^2.
- Compared to the LPV module, the performance ratio of the PSFPV was improved up to 23.00% by increasing the submerged ratio to 12%.
- The mitigation of CO_2 emission per summer season attributable to the operation of the PSFPV system on water reservoirs can alleviate the CO_2 emissions by about 49.66 kg CO_2.
- The estimated LCOE for both systems reveals that by increasing the submerged ratio from 4% to 12%, LCOEs of 0.075 $/kWh, and 0.067 $/kWh were reached for the PSFPV system respectively.

After accounting for the benefit of reduced evaporation, the PFSPV system outperforms in terms of productivity and financial statements; consequently, this study contributes to the development of the floating photovoltaics system by immersing it in various accessible water bodies.

4. Recommendation for future work

The floating PV system is, in fact, a novel modified energy generation technology. The research presented in this work only addresses the core challenges of the FPV productivity enhancement concept; other concerns, such as evaporation reduction, would need to be addressed in future work.

Acknowledgment

This study was funded by Egypt-UK Cooperation: Newton-Mosharafa Program: Researcher Links: Institutional Links (STDF) [grant number ID/42715] and Port Said University. The authors would like to express their gratitude to (STDF) for their fund and Port Said University for their support.

References

[1] IRENA. Global energy transformation: A roadmap to 2050 (2019 edition). 2019.

[2] Wang RZ, Zhai XQ. Development of solar thermal technologies in China. Energy 2010;35:4407–16. https://doi.org/10.1016/j.energy.2009.04.005.

[3] Tonui JK, Tripanagnostopoulos Y. Improved PV/T solar collectors with heat extraction by forced or natural air circulation. Renewable Energy 2007;32:623–37. https://doi.org/10.1016/j.renene.2006.03.006.

[4] Koteswararao B, Radha Krishna K, Vijay P, Raja Surya N. Experimental Analysis of solar panel efficiency with different modes of cooling. International Journal of Engineering and Technology 2016;8:1451–6.

[5] Maleki A, Haghighi A, El Haj Assad M, Mahariq I, Alhuyi Nazari M. A review on the approaches employed for cooling PV cells. Solar Energy 2020;209:170–85. https://doi.org/10.1016/j.solener.2020.08.083.

[6] Siah Chehreh Ghadikolaei S. Solar photovoltaic cells performance improvement by cooling technology: An overall review. International Journal of Hydrogen Energy 2021;46:10939–72. https://doi.org/10.1016/j.ijhydene.2020.12.164.

[7] Shah TR, Babar H, Ali HM. Chapter 8 - Energy harvesting: role of hybrid nanofluids. In: Ahmed W, Booth M, Nourafkan EBT-EN for RE, editors. Micro and Nano Technologies, Elsevier; 2021, p. 173–211. https://doi.org/https://doi.org/10.1016/B978-0-12-821346-9.00011-0.

[8] Sargunanathan S, Elango A, Mohideen ST. Performance enhancement of solar photovoltaic cells using effective cooling methods: A review. Renewable and Sustainable Energy Reviews 2016;64:382–93. https://doi.org/10.1016/j.rser.2016.06.024.

[9] Sajjad U, Amer M, Ali HM, Dahiya A, Abbas N. Cost effective cooling of photovoltaic modules to improve efficiency. Case Studies in Thermal Engineering 2019;14:100420. https://doi.org/10.1016/j.csite.2019.100420.

[10] Bayrak F, Oztop HF, Selimefendigil F. Experimental study for the application of different cooling techniques in photovoltaic (PV) panels. Energy Conversion and Management 2020;212:112789. https://doi.org/10.1016/j.enconman.2020.112789.

[11] Amr AA raheim, Hassan AAM, Abdel-Salam M, El-Sayed AHM. Enhancement of photovoltaic system performance via passive cooling: Theory versus experiment. Renewable Energy 2019;140:88–103. https://doi.org/10.1016/j.renene.2019.03.048.

[12] Idoko L, Anaya-Lara O, McDonald A. Enhancing PV modules efficiency and power output using multi-concept cooling technique. Energy Reports 2018;4:357–69. https://doi.org/https://doi.org/10.1016/j.egyr.2018.05.004.

[13] Hernandez-Perez JG, Carrillo JG, Bassam A, Flota-Banuelos M, Patino-Lopez LD. A new passive PV heatsink design to reduce efficiency losses: A computational and experimental evaluation. Renewable Energy 2020;147:1209–20. https://doi.org/10.1016/j.renene.2019.09.088.

[14] Abdollahi N, Rahimi M. Potential of water natural circulation coupled with nano-enhanced PCM for PV module cooling. Renewable Energy 2020;147:302–9. https://doi.org/10.1016/j.renene.2019.09.002.

[15] Caglar B, Araz M, Ozcan HG, Calisan A, Hepbasli A. Energy and exergy analysis of a PV-T integrated ethanol PEM electrolyzer. International Journal of Hydrogen Energy 2021;46:12615–38. https://doi.org/10.1016/j.ijhydene.2021.01.055.

[16] Sahu A, Yadav N, Sudhakar K. Floating photovoltaic power plant: A review. Renewable and Sustainable Energy Reviews 2016;66:815–24.

https://doi.org/10.1016/j.rser.2016.08.051.
[17] Trapani K, Millar DL. Proposing offshore photovoltaic (PV) technology to the energy mix of the Maltese islands. Energy Conversion and Management 2013;67:18–26. https://doi.org/10.1016/j.enconman.2012.10.022.
[18] Cazzaniga R, Cicu M, Rosa-Clot M, Rosa-Clot P, Tina GM, Ventura C. Floating photovoltaic plants: Performance analysis and design solutions. Renewable and Sustainable Energy Reviews 2018;81:1730–41. https://doi.org/10.1016/j.rser.2017.05.269.
[19] Choi JW, Seo SH, Joo HJ, Yoon SJ. Structural Performance Evaluation of Floating PV Power Generation Structure System. Journal of The Korean Society of Civil Engineers 2014;34:1353–62. https://doi.org/10.12652/ksce.2014.34.5.1353.
[20] Choi Y-K. A Study on Power Generation Analysis of Floating PV System Considering Environmental Impact. International Journal of Software Engineering and Its Applications 2014;8:75–84. https://doi.org/10.14257/ijseia.2014.8.1.07.
[21] Tsoutsos T, Frantzeskaki N, Gekas V. Environmental impacts from the solar energy technologies. Energy Policy 2005;33:289–96. https://doi.org/10.1016/S0301-4215(03)00241-6.
[22] Ates AM, Yilmaz OS, Gulgen F. Using remote sensing to calculate floating photovoltaic technical potential of a dam's surface. Sustainable Energy Technologies and Assessments 2020;41:100799. https://doi.org/10.1016/j.seta.2020.100799.
[23] Mittal D, Kumar Saxena B, Rao KVS. Potential of floating photovoltaic system for energy generation and reduction of water evaporation at four different lakes in Rajasthan. Proceedings of the 2017 International Conference On Smart Technology for Smart Nation, SmartTechCon 2017, Institute of Electrical and Electronics Engineers Inc.; 2018, p. 238–43. https://doi.org/10.1109/SmartTechCon.2017.8358376.
[24] Liu L, Wang Q, Lin H, Li H, Sun Q, Wennersten R. Power Generation Efficiency and Prospects of Floating Photovoltaic Systems. Energy Procedia 2017;105:1136–42. https://doi.org/10.1016/j.egypro.2017.03.483.
[25] Temiz M, Javani N. Design and analysis of a combined floating photovoltaic system for electricity and hydrogen production. International Journal of Hydrogen Energy 2020;45:3457–69. https://doi.org/10.1016/j.ijhydene.2018.12.226.
[26] Muhammad A, Muhammad U, Abid Z. Potential of floating photovoltaic technology in Pakistan. Sustainable Energy Technologies and Assessments 2021;43:100976. https://doi.org/10.1016/j.seta.2020.100976.
[27] Hasan A, Dincer I. A new performance assessment methodology of bifacial photovoltaic solar panels for offshore applications. Energy Conversion and Management 2020;220:112972. https://doi.org/10.1016/j.enconman.2020.112972.
[28] Luo W, Isukapalli SN, Vinayagam L, Ting SA, Pravettoni M, Reindl T, et al. Performance loss rates of floating photovoltaic installations in the tropics. Solar Energy 2021:1–7. https://doi.org/10.1016/j.solener.2020.12.019.
[29] El Hammoumi A, Chalh A, Allouhi A, Motahhir S, El Ghzizal A, Derouich A. Design and construction of a test bench to investigate the potential of floating PV systems. Journal of Cleaner Production 2020;278:123917. https://doi.org/10.1016/j.jclepro.2020.123917.
[30] Dai J, Zhang C, Lim HV, Ang KK, Qian X, Wong JLH, et al. Design and construction of floating modular photovoltaic system for water reservoirs. Energy 2020;191:116549. https://doi.org/10.1016/j.energy.2019.116549.
[31] Kaymak MK, Şahin AD. Problems encountered with floating photovoltaic systems under real conditions: A new FPV concept and novel solutions. Sustainable Energy

Technologies and Assessments 2021;47:101504. https://doi.org/10.1016/j.seta.2021.101504.
[32] Cazzaniga R, Cicu M, Rosa-Clot M, Rosa-Clot P, Tina GM, Ventura C. Compressed air energy storage integrated with floating photovoltaic plant. Journal of Energy Storage 2017;13:48–57. https://doi.org/10.1016/j.est.2017.06.006.
[33] Rosa-Clot M, Rosa-Clot P, Tina GM, Scandura PF. Submerged photovoltaic solar panel: SP2. Renewable Energy 2010;35:1862–5. https://doi.org/10.1016/j.renene.2009.10.023.
[34] Goswami A, Sadhu P, Goswami U, Sadhu PK. Floating solar power plant for sustainable development: A techno-economic analysis. Environmental Progress and Sustainable Energy 2019;38. https://doi.org/10.1002/ep.13268.
[35] Gonzalez Sanchez R, Kougias I, Moner-Girona M, Fahl F, Jäger-Waldau A. Assessment of floating solar photovoltaics potential in existing hydropower reservoirs in Africa. Renewable Energy 2021;169:687–99. https://doi.org/10.1016/j.renene.2021.01.041.
[36] Kumar NM, Subramaniam U, Mathew M, Ajitha A, Almakhles DJ. Exergy analysis of thin-film solar PV module in ground-mount, floating and submerged installation methods. Case Studies in Thermal Engineering 2020;21:100686. https://doi.org/10.1016/j.csite.2020.100686.
[37] Lanzafame R, Nachtmann S, Rosa-Clot M, Rosa-Clot P, Scandura PF, Taddei S, et al. Field experience with performances evaluation of a single-crystalline photovoltaic panel in an underwater environment. IEEE Transactions on Industrial Electronics 2010;57:2492–8. https://doi.org/10.1109/TIE.2009.2035489.
[38] China completes largest floating solar power plant - PV Tech n.d. https://www.pv-tech.org/china-completes-largest-floating-solar-power-plant/ (accessed September 26, 2021).
[39] Mizukoshi K, Yamamura T, Tomioka Y, Kawamura M. Optimization of lowermost layer material for low-resistivity Ag-based multilayer structure in low-emissivity glass. Thin Solid Films 2021;739:138996. https://doi.org/10.1016/j.tsf.2021.138996.
[40] Salem MR, Ali RK, Elshazly KM. Experimental investigation of the performance of a hybrid photovoltaic/thermal solar system using aluminium cooling plate with straight and helical channels. Solar Energy 2017;157:147–56. https://doi.org/10.1016/j.solener.2017.08.019.
[41] Xiaoping L, Yunyou Q, SaeidNahaei S. A novel maximum power point tracking in partially shaded PV systems using a hybrid method. International Journal of Hydrogen Energy 2021;46:37351–66. https://doi.org/10.1016/j.ijhydene.2021.08.202.
[42] Bashir MA, Ali HM, Khalil S, Ali M, Siddiqui AM. Comparison of performance measurements of photovoltaic modules during winter months in Taxila, Pakistan. International Journal of Photoenergy 2014;2014. https://doi.org/10.1155/2014/898414.
[43] Elminshawy NAS, Gadalla MA, Bassyouni M, El-Nahhas K, Elminshawy A, Elhenawy Y. A novel concentrated photovoltaic-driven membrane distillation hybrid system for the simultaneous production of electricity and potable water. Renewable Energy 2020;162:802–17. https://doi.org/10.1016/j.renene.2020.08.041.
[44] Abd Elbar AR, Hassan H. An experimental work on the performance of new integration of photovoltaic panel with solar still in semi-arid climate conditions. Renewable Energy 2020;146:1429–43. https://doi.org/10.1016/j.renene.2019.07.069.
[45] Elminshawy A, Morad K, Elminshawy NAS, Elhenawy Y. Performance enhancement of concentrator photovoltaic systems using nanofluids. International Journal of Energy Research 2021;45:2959–79. https://doi.org/10.1002/er.5991.

[46] Wang X, Sun P, Tang Y, Liang Z. Distribution Characteristics of Fat Greenling (Hexagrammos otakii) Inhabiting Artificial Reefs Around Qiansandao Island, Haizhou Bay, China. Journal of Ocean University of China 2019;18:1227–34. https://doi.org/10.1007/s11802-019-4010-7.
[47] Elminshawy NAS, Osama A, El-Damhogi DG, Oterkus E, Mohamed AMI. Simulation and experimental performance analysis of partially floating PV system in windy conditions. Solar Energy 2021;230:1106–21. https://doi.org/10.1016/j.solener.2021.11.020.
[48] Liu Z, Yu Z (Jerry), Yang T, Li S, El Mankibi M, Roccamena L, et al. Experimental investigation of a vertical earth-to-air heat exchanger system. Energy Conversion and Management 2019;183:241–51. https://doi.org/10.1016/j.enconman.2018.12.100.
[49] Elminshawy NAS, Ghandour M El, Gad HM, El-Damhogi DG, El-Nahhas K, Addas MF. The performance of a buried heat exchanger system for PV panel cooling under elevated air temperatures. Geothermics 2019;82:7–15. https://doi.org/https://doi.org/10.1016/j.geothermics.2019.05.012.
[50] Montes MJ, Rovira A, Muñoz M, Martínez-Val JM. Performance analysis of an Integrated Solar Combined Cycle using Direct Steam Generation in parabolic trough collectors. Applied Energy 2011;88:3228–38. https://doi.org/10.1016/j.apenergy.2011.03.038.
[51] Shen W, Chen X, Qiu J, Hayward JA, Sayeef S, Osman P, et al. A comprehensive review of variable renewable energy levelized cost of electricity. Renewable and Sustainable Energy Reviews 2020;133:110301. https://doi.org/10.1016/j.rser.2020.110301.
[52] Said M, EL-Shimy M, Abdelraheem MA. Photovoltaics energy: Improved modeling and analysis of the levelized cost of energy (LCOE) and grid parity - Egypt case study. Sustainable Energy Technologies and Assessments 2015;9:37–48. https://doi.org/10.1016/j.seta.2014.11.003.
[53] Sharma HB, Panigrahi S, Sarmah AK, Dubey BK. Jo ur na l P re of. Journal of Cleaner Production 2021:135907. https://doi.org/10.1016/j.jclepro.2021.126117.
[54] Ali HM. A semi-empirical model for retained condensate on horizontal pin-fin tube including the effect of vapour velocity. Case Studies in Thermal Engineering 2021;28:101420. https://doi.org/10.1016/j.csite.2021.101420.
[55] Gorjian S, Sharon H, Ebadi H, Kant K, Scavo FB, Tina GM. Recent technical advancements, economics and environmental impacts of floating photovoltaic solar energy conversion systems. Journal of Cleaner Production 2021;278:124285. https://doi.org/10.1016/j.jclepro.2020.124285.
[56] Rajput P, Tiwari GN, Sastry OS. Thermal modelling with experimental validation and economic analysis of mono crystalline silicon photovoltaic module on the basis of degradation study. Energy 2017;120:731–9. https://doi.org/https://doi.org/10.1016/j.energy.2016.11.123.
[57] Baloch AAB, Bahaidarah HMS, Gandhidasan P, Al-Sulaiman FA. Experimental and numerical performance analysis of a converging channel heat exchanger for PV cooling. Energy Conversion and Management 2015;103:14–27. https://doi.org/10.1016/j.enconman.2015.06.018.
[58] Duffley P, Larrivée P. Whatever floats your boat: A corpus-based investigation of definiteness, quantification, modality, presuppositional content, scalarity and epistemic stance with wh-ever words. International Review of Pragmatics 2020;12:206–45. https://doi.org/10.1163/18773109-01202002.
[59] Oliveira-Pinto S, Stokkermans J. Assessment of the potential of different floating solar

technologies – Overview and analysis of different case studies. Energy Conversion and Management 2020;211:112747. https://doi.org/10.1016/j.enconman.2020.112747.
[60] Elminshawy NAS, El-Ghandour M, Elhenawy Y, Bassyouni M, El-Damhogi DG, Addas MF. Experimental investigation of a V-trough PV concentrator integrated with a buried water heat exchanger cooling system. Solar Energy 2019;193:706–14. https://doi.org/10.1016/j.solener.2019.10.013.
[61] Elminshawy NAS, Mohamed AMI, Morad K, Elhenawy Y, Alrobaian AA. Performance of PV panel coupled with geothermal air cooling system subjected to hot climatic. Applied Thermal Engineering 2019;148:1–9. https://doi.org/10.1016/j.applthermaleng.2018.11.027.
[62] Martins BP. Techno-economic evaluation of a floating PV system for a wastewater treatment facility. KTH School of Industrial Engineering and Management Energy, 2019.
[63] IFC. Utility-Scale Solar Photovoltaic Power Plants. 2015.
[64] Rosa-Clot M, Tina GM. Chapter 8 - Floating Plants and Environmental Aspects. In: Rosa-Clot M, Tina GMBT-S and FPS, editors., Academic Press; 2018, p. 185–212. https://doi.org/https://doi.org/10.1016/B978-0-12-812149-8.00009-0.
[65] Barbuscia M. Economic viability assessment of floating photovoltaic energy. Working Paper 2018;1:1–11.